ARTICLES
https://doi.org/10.1038/s41559-021-01548-3

nature ecology & evolution

Global hunter-gatherer population densities constrained by influence of seasonality on diet composition

Dan Zhu[1,2]✉, Eric D. Galbraith[3,2,4], Victoria Reyes-García[2,4] and Philippe Ciais[5,6]

The dependence of hunter-gatherers on local net primary production (NPP) to provide food played a major role in shaping long-term human population dynamics. Observations of contemporary hunter-gatherers have shown an overall correlation between population density and annual NPP but with a 1,000-fold variation in population density per unit NPP that remains unexplained. Here, we build a process-based hunter-gatherer population model embedded within a global terrestrial biosphere model, which explicitly addresses the extraction of NPP through dynamically allocated hunting and gathering activities. The emergent results reveal a strong, previously unrecognized effect of seasonality on population density via diet composition, whereby hunter-gatherers consume high fractions of meat in regions where growing seasons are short, leading to greatly reduced population density due to trophic inefficiency. This seasonal carnivory bottleneck largely explains the wide variation in population density per unit NPP and questions the prevailing usage of annual NPP as the proxy of carrying capacity for ancient humans. Our process-based approach has the potential to greatly refine our understanding of dynamical responses of ancient human populations to past environmental changes.

Hunter-gatherer populations, that subsist on hunting, gathering and fishing, rely intimately on the biotic fabrics of their local environments[1–3]. Although only a handful of hunter-gatherer populations remain, over 300 societies of contemporary hunter-gatherers have been documented sporadically over the past two centuries[1]. Due to the assumed similarities between their lifestyles and those of our foraging ancestors, contemporary hunter-gatherers have provided many insights about our species' past[4–8], informing reconstructions of population changes on evolutionary timescales[5,6], the timing and rates of global human dispersals[4,7] and the drivers behind the origin of agriculture[8]. Yet, these contemporary societies do not provide direct analogues of ancient foragers, as they have had more complex technologies[9] and had experienced interactions with and pressures from neighbouring agricultural and industrial societies[10,11], such as acquiring supplemental agricultural food[2,12] or encountering novel pathogens near the time of documentation, which may have modulated the population density–ecosystem relationships. Thus, many of the observational data may provide distorted views of the pre-existing state, casting doubt on statistical models and demographic parameters that are directly fitted to the contemporary data[5–8]. Taking full advantage of the insights from contemporary hunter-gatherers requires a mechanistic, process-oriented understanding of how environmental factors influence the distribution and abundance of hunter-gatherer populations.

Because hunter-gatherers acquire food directly from their surrounding environment, it has long been thought that their population density should be closely linked to the productivity of their local ecosystems[1,2] and numerous studies have used net primary production (NPP) as the main predictor for ancient hunter-gatherer density changes[4,7,13]. However, although contemporary hunter-gatherer population density is positively correlated with NPP, NPP alone explains <30% of the variability of population density (Fig. 1a). The fraction of NPP consumed by hunter-gatherers (Φ_{NPP}; Methods), which also indicates population density per unit NPP, varies by three orders of magnitude across the recorded groups (Fig. 1b and Supplementary Fig. 1e). A portion of this scatter could reflect the confounding historical influences but it has also been assumed that the edible proportion of primary production differs among biomes[2]. However, our analysis does not show systematic differences in Φ_{NPP} between biome categories, except for a lower Φ_{NPP} in boreal forest and a marginally significantly higher Φ_{NPP} in Mediterranean forest (Fig. 1b and Supplementary Fig. 2b). Nor does Φ_{NPP} show a consistent change across the NPP gradient (Supplementary Fig. 2c). The wide spread in Φ_{NPP} thus remains unexplained. The weak statistical dependence of population density on NPP has prompted a recourse to other explanatory variables, including biodiversity[3], pathogen stress[3], precipitation seasonality[8], climate variability[14] and social complexity-related variables such as food storage-dependence[14]. It is, however, difficult to tease apart the causality among these intercorrelated variables using statistical methods alone.

Here, we build a mechanistic understanding of hunter-gatherer populations with a global, activity-based process model for which population density is an emergent feature. Our model operates within the framework of an Earth system model (ESM) (Fig. 2). During the past decades, the land components of ESMs have integrated vegetation modules to resolve key processes of biogeochemical cycling of carbon, energy and water[15] and have recently begun to incorporate large mammalian herbivores on the basis of

[1]Sino-French Institute for Earth System Science, College of Urban and Environmental Sciences, Peking University, Beijing, China. [2]Institut de Ciència i Tecnologia Ambientals (ICTA-UAB), Universitat Autònoma de Barcelona, Barcelona, Spain. [3]Department of Earth and Planetary Sciences, McGill University, Montreal, Quebec, Canada. [4]ICREA (Catalan Institution for Research and Advanced Studies), Barcelona, Spain. [5]Laboratoire des Sciences du Climat et de l'Environnement, IPSL-LSCE, CEA-CNRS-UVSQ-UPSACLAY, Gif sur Yvette, France. [6]Climate and Atmosphere Research Center (CARE-C), The Cyprus Institute, Nicosia, Cyprus. ✉e-mail: zhudan@pku.edu.cn

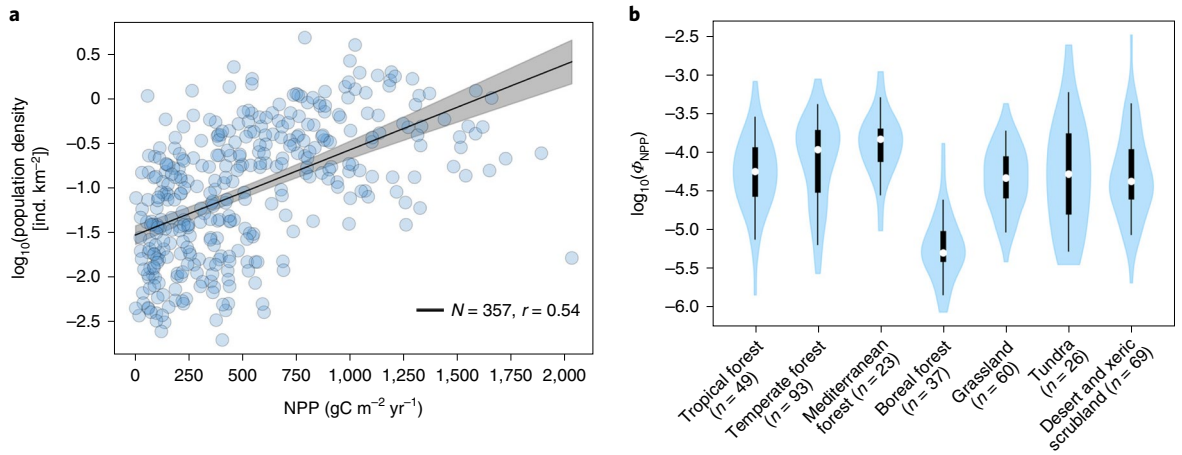

Fig. 1 | Contemporary hunter-gatherer population density versus net primary production. a, Relationship between population density, from ethnographic records at 357 locations (Supplementary Fig. 1) and NPP, according to the MODIS satellite-derived product (Methods). The solid line gives the linear regression of $\log_{10}$(population density) versus NPP ($y = 9.6 \times 10^{-4}x - 1.53$) with 95% confidence intervals (CIs) shown in grey. **b**, Violin plot for Φ_{NPP} (fraction of NPP consumed by hunter-gatherers, calculated as population density multiplied by a constant intake rate and divided by NPP; Methods) of populations located in different biomes (Supplementary Fig. 2). The white circles represent median values and the thick (and thin) black bars the interquantile (and 5th–95th) ranges. Except for a lower Φ_{NPP} in boreal forest and a slightly higher Φ_{NPP} in Mediterranean forest, Φ_{NPP} does not differ significantly among the other five biome types (analysis of variance test $P > 0.05$).

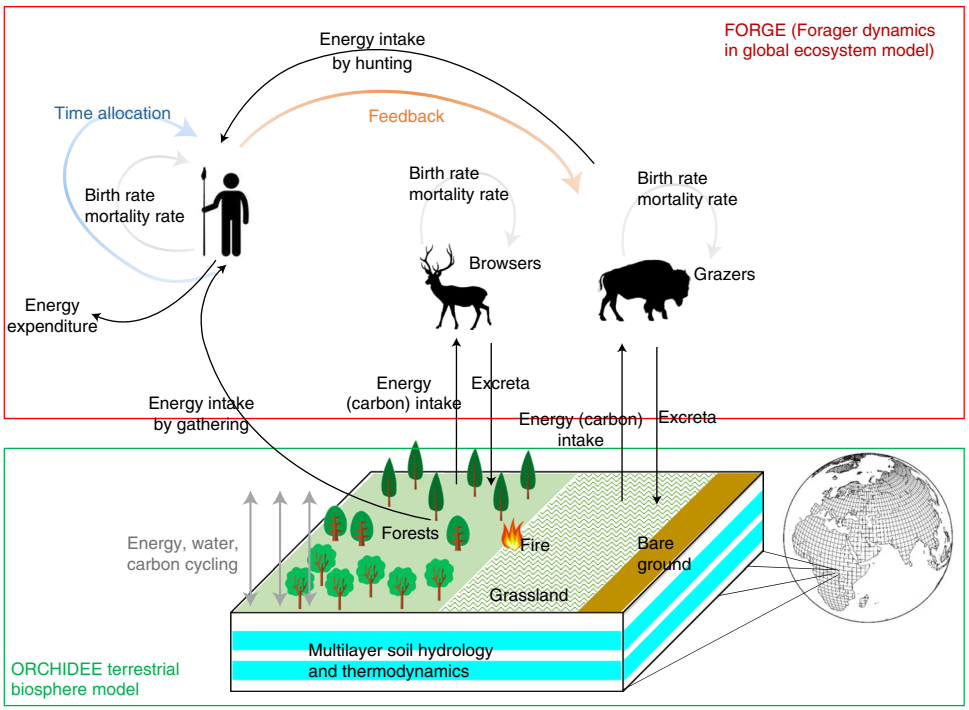

Fig. 2 | Schematic of FORGE, coupled to the ORCHIDEE global terrestrial biosphere model. FORGE simulates daily energy (carbon) intake from plants and animals and energy expenditure (black arrows); these energy in/out-fluxes update an energetic reserve pool (body fat) every day, which indicates the average health state and then impacts birth rate and mortality rate, determining changes in hunter-gatherer population density every year. The daily intake rate depends on food abundance and on the time spent in hunting and gathering, calculated with time allocation algorithms (Methods).

metabolic and demographic equations[16,17]. Our model directly couples human population dynamics to such a land model[17], simulating human time allocation to hunting versus gathering in response to the interaction between humans and food resources (Methods). The model uses explicit formulations of daily carbon/energy flows among vegetation, herbivores and humans, the outcome of which determines human reproduction and mortality rates. These fluxes depend on a time allocation scheme with two simple assumptions: first, total foraging time increases or decreases depending on the level of fullness of the previous day; and second, gathering versus hunting time depends on the relative abundance of plant versus animal food and on an underlying a priori preference for meat. The model is resolved on a daily time step, thus capturing the seasonal cycle in high detail.

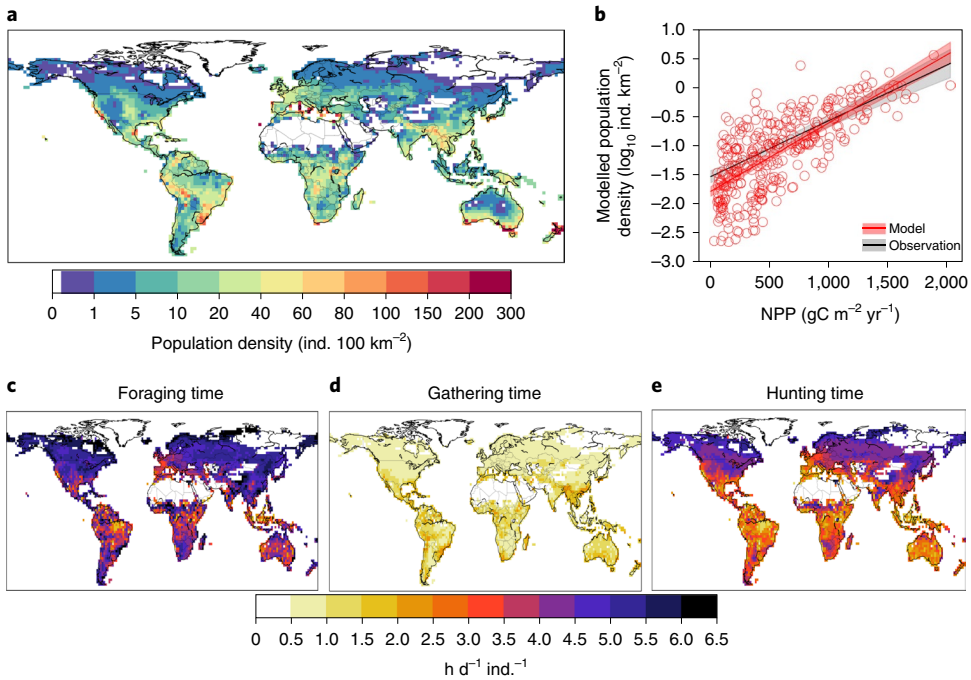

Fig. 3 | Modelled population density and time allocation. a, Map of hunter-gatherer population density equilibrated under present-day climate (results in the S2 experiment; Methods). **b**, Relationship between population density and NPP at the grid cells where the observational data are located. The red solid line indicates linear regression of $\log_{10}$(population density) versus NPP ($y = 11.7 \times 10^{-4}x - 1.78$, $n = 334$, $r = 0.72$), with 95% CIs shown in red shading. For comparison, regression of the observations is shown in grey (same as those in Fig. 1a). **c–e**, Modelled time spent in foraging (**c**), separated into gathering (**d**) and hunting (**e**). The grid cells where modelled population density is <0.2 ind. 100 km^{-2} are shown in white in the maps and excluded in **b**.

Results

Modelled global distribution of hunter-gatherers. Simulated steady-state global population density and foraging times under present-day climate are shown in Fig. 3. The model simulates high densities in most regions with high NPP and closely matches the observed relationship of density versus NPP derived from contemporary hunter-gatherer data (Fig. 3b). Simulated foraging times are generally 3.5–5.5 h per person per day throughout the world, close to the average of available observations from a few hunter-gatherer groups[2,18,19] (~4 hours per day per individual [h d^{-1} ind.$^{-1}$]). In the model, slightly more time is spent hunting than gathering in the tropics, whereas most of the foraging time is devoted to hunting at high latitudes (Fig. 3c–e).

The simulated population density agrees reasonably well with the ethnographic data (Pearson correlation coefficient $r = 0.58$; Supplementary Fig. 3a,b) and there is also a strong correlation between simulated and ethnographically recorded diet compositions, although less of the observed variance is explained ($r = 0.40$ for the meat fraction of the diet; Supplementary Fig. 3c,d). Model-data discrepancies may be partly due to the lack of fishing in the model, which is a major source of food in many coastal societies (Supplementary Fig. 1d). In addition, the model treats all plant or animal food equally, thus ignoring the wide variety such as the different energy content, protein richness and relative abundance of each food item within both broad categories[2,20–22]. Any bias in the vegetation and herbivore dynamics model[17] could also propagate to the human model, contributing to the model-data mismatch (note that the S2 experiment has corrected part of the biases in the vegetation inputs to the FORGE (Forager dynamics in Global Ecosystem) model; Methods). Furthermore, discrepancies could arise from climate shifts and non-steady-state factors, given that the model simulates equilibrium densities forced by present-day climate (while the ethnographic records were collected during the past 200 years[1]) whereas some of the populations were under positive growth rate when being studied[23]. There are also important uncertainties in the diet composition data, as the estimation methods for the amounts of gathered, hunted and fished food are often inconsistent, sometimes measured in different units (weight or calorie) and occasionally based on the ethnographers' impressions[2], which may further add to the model-data scatter.

The modelled global total hunter-gatherer population is 17 million, which is at the high end of the estimates of prehistoric (pre-agriculture) population derived by extrapolating national historical records, which range from 1 million to 20 million[24]. This can be partly explained by the fact that our model was calibrated with data from contemporary hunter-gatherers, who presumably had more advanced technologies and access to non-local foods than did early-Holocene foragers[25] (Supplementary Discussion 2 gives the test runs regarding the technology-dependent foraging efficiency parameter). Geographical differences also contribute to our estimate being higher than previous upscalings of contemporary hunter-gatherer populations, which include regression models (10–12 million; refs. [3,26]) and a proportional projection method (7 million; ref. [1]). For the former, the difference is primarily attributable to a higher density in Africa and southern Asia in our model (Supplementary Fig. 4), where the populations were suppressed in ref. [3] due to a high pathogen stress as a predictor in their regression (Supplementary Discussion 1 gives more on pathogen stress). For the latter, we find that the global estimate with the same projection method but a different upscaling biome map ranges from 10 million to 17 million, contingent on how an average population density is calculated for each biome (Supplementary Discussion 3). Therefore, we consider our result of 17 million, simulated by a process-based model, to be a reasonable, independent estimate of potential global hunter-gatherer population size under modern climate with advanced foraging technology, assuming foraging as the only subsistence type.

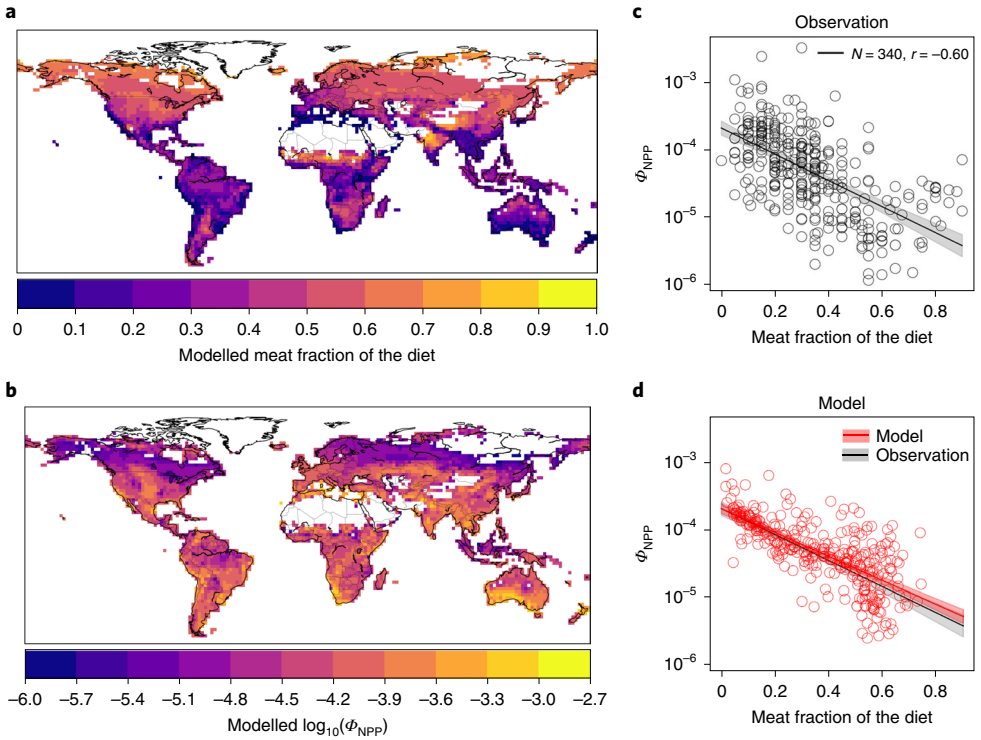

Fig. 4 | Meat fraction of the diet controls Φ_{NPP}. a,**b**, Modelled fraction of hunted food in the diet (**a**) and Φ_{NPP} (fraction of NPP consumed by hunter-gatherers) (**b**). **c**,**d**, Relationship between Φ_{NPP} and meat fraction of the diet according to ethnographic records (**c**) and model results (**d**). The black and red solid lines give the linear regressions of $\log_{10}(\Phi_{NPP})$ versus meat fraction from observations (**c**) ($y = -1.93x - 3.68$) and the model (**d**) ($y = -1.78x - 3.68$, $n = 334$, $r = -0.73$), with 95% CIs shown in shading. The grid cells where modelled population density is <0.2 ind. 100 km^{-2} are shown in white in the maps and excluded in **d**.

Linkage among seasonality, diet composition and population density. As in the observations, simulated Φ_{NPP} (fraction of NPP consumed by hunter-gatherers) displays a huge spatial variation with a 1,000-fold range (Fig. 4b). The spatial distribution of Φ_{NPP} follows an inverse relationship with the meat fraction of the diet (compare Fig. 4a,b). The negative correlation is clear in the scatter plot, both for grid cells where the observational data are located (Fig. 4d) and for all populated grid cells in the model (Supplementary Fig. 5), showing a drop of Φ_{NPP} by almost an order of magnitude as meat fraction increases by 60%. Remarkably, this emergent property of the model is corroborated by ethnographic data, which fall over a comparable range (compare Fig. 4c,d). Indeed, in both the observations and the model, a higher meat fraction of the diet is associated with a lower population density under the same level of NPP (Supplementary Fig. 6). It is possible that the use of aquatic resources, which are not included explicitly in the model, could increase the density of some populations relative to terrestrial NPP (and thus Φ_{NPP}) and thus confound the model-observation comparison. However, we checked that the observed correlation between Φ_{NPP} and meat fraction holds when the groups with fish-rich diets are excluded (Supplementary Fig. 7). Therefore, although aquatic resources are important for hunter-gatherers in some locations (Supplementary Fig. 1d), the association between Φ_{NPP} and meat fraction appears to be a robust feature of the observations. Notably, even the groups with intermediate ($30\% \leq$ fishing $< 50\%$) or high ($\geq 50\%$) fishing percentages display significant negative correlations between Φ_{NPP} and meat fraction as well (Supplementary Fig. 7), lending confidence to this overall trend.

The meat fraction of the modelled hunter-gatherer diet is mainly driven by a scarcity of vegetation edible by humans during winter or dry seasons in the model. In regions with relatively small seasonal variations in NPP, foragers can subsist mainly on gathering throughout the year due to a substantially higher abundance of plant food than animal food at equilibrium (Fig. 5a). By contrast, in regions with long non-growing seasons, edible plant biomass becomes depleted and foragers depend on hunting to subsist through the season of scarcity. As a result, the production rate of animals imposes a strong constraint on human population density in regions with short growing seasons, regardless of how abundant plant food may be during the growing season (Fig. 5b). Since relatively little energy flows from primary to secondary production due to trophic inefficiency (Fig. 5), the Φ_{NPP} is expected to be lower for humans subsisting more on animals. Therefore, the apparent negative correlation between Φ_{NPP} and meat fraction (Fig. 4d and Supplementary Fig. 5) is caused both directly by the effect of shifts in humans' trophic position and indirectly by the covariation between meat fraction and seasonality, the latter being able to influence Φ_{NPP} through the limiting seasonal minima.

With the process-based model, we quantify the contribution of the two effects, by conducting two experiments in which humans only subsist on either plants or animals (via allocating all foraging time in either gathering or hunting, hereafter 'onlyGather' and 'onlyHunt'). The difference in the resultant Φ_{NPP} between the two runs could be regarded as the direct impact of the trophic position. In the results of onlyGather, humans only persist in regions with long growing seasons (>~180 d) but the total population size in these populated areas is 9.5 times higher than that in the onlyHunt experiment for the same area (Supplementary Fig. 8). Correspondingly, Φ_{NPP} is mostly higher in onlyGather than in onlyHunt (albeit the opposite occurs in a few grid cells with relatively shorter growing seasons where a full reliance on hunting slightly increases population density) and $\log_{10}(\Phi_{NPP})$ increases by 0.85 (or Φ_{NPP} increases

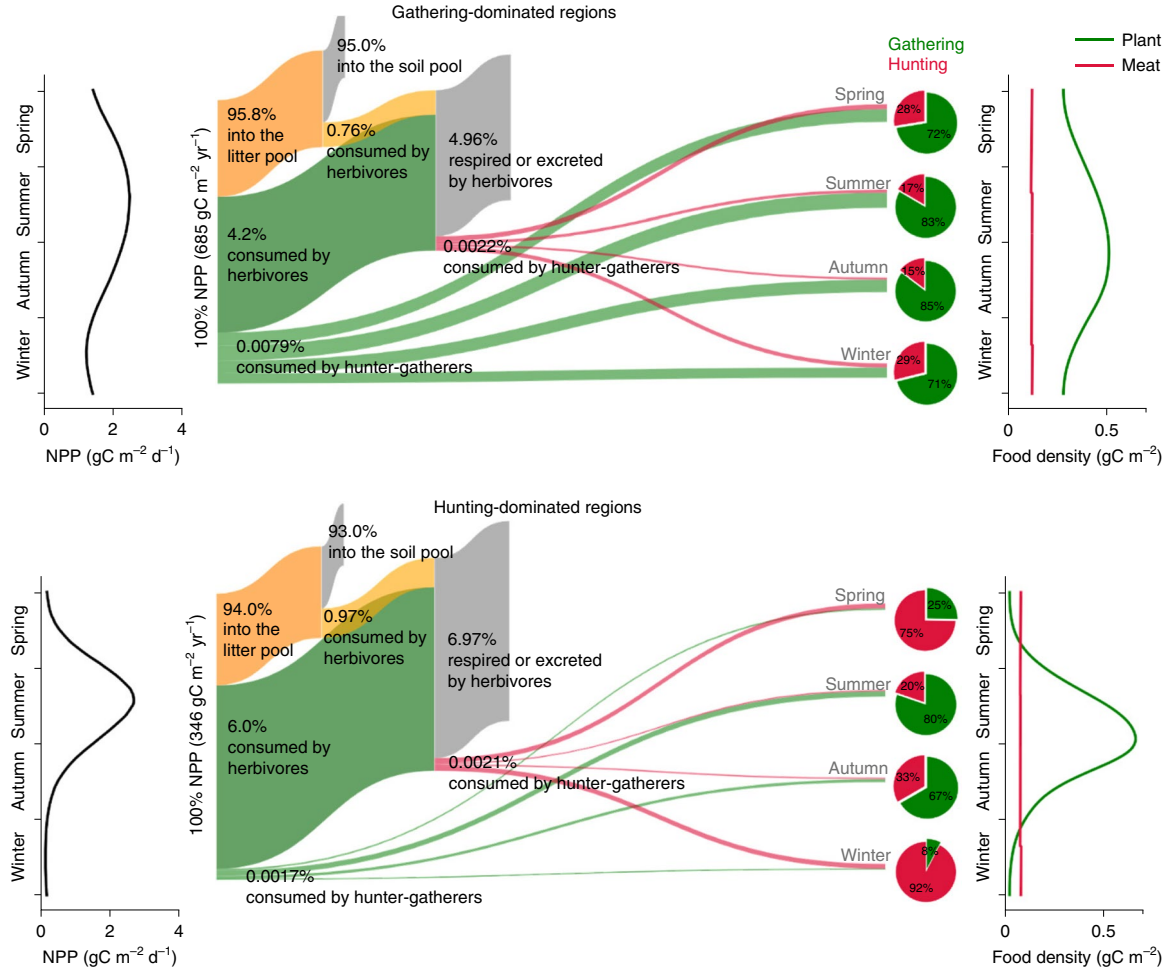

Fig. 5 | Seasonality, diet composition and carbon flows. Model results were averaged over all grid cells of either gathering-dominated (modelled annual mean hunted food <40%; Fig. 4a) or hunting-dominated (hunted food ≥40%) regions, at dynamic equilibrium. Mean population density of the two regions is 0.19 and 0.04 ind. km^{-2} and mean meat fraction of the diet is 22 and 55%, respectively. To synchronize the seasonal cycles between the two hemispheres, outputs of the southern hemisphere were shifted by 6 months. The numbers on the links indicate percentages of annual NPP that flow to herbivores, humans and litter (dead plants) and soil pools. Note that for legibility, the link widths are not strictly proportional to the magnitude of flows. Spring, March, April, May; Summer, June, July, August; Autumn, September, October, November; Winter, December, January, February.

by seven times) on average in onlyGather compared to onlyHunt (Supplementary Fig. 8e). Therefore, the direct effect of diet composition via trophic energetics contributes about half to the apparent slope of Φ_{NPP} versus meat fraction.

The modelled contrast of seasonal cycles in diet composition between long versus short growing season regions (Fig. 5) is qualitatively supported by observations in the Ache (in tropical forest)[20] and in the Hiwi (in savanna)[27] and Bushmen groups (in Kalahari desert)[28]. The first group, living in places with relatively high NPP all year round, exhibits little seasonal variance in both meat and plant intake, whereas the last two groups, living in highly seasonal environments, exhibit a highly varied share of plant food across seasons. An in-depth quantitative evaluation is, however, difficult due to the limited number of hunter-gatherer groups with detailed, seasonally based diet records and because the model cannot capture the highly diverse phenology of various plant and animal species at the local ecosystems.

Given the strong role of meat fraction in controlling population density predicted by the process-based model, we carried out a statistical analysis of contemporary hunter-gatherer data to test if meat fraction emerges as a significant predictor (Supplementary Discussion 1). Our analysis shows that, indeed, a multivariable stepwise linear regression with nine empirical predictors (NPP, tree and grass coverage, biodiversity, growing season length, percentages of food derived from hunting, gathering and fishing and absolute latitude) identifies the hunting percentage as the strongest explanatory variable for population density, followed by NPP and grass cover, while the other variables are non-significant. Hunting percentage itself can be explained by growing season length, followed by grass coverage (Supplementary Discussion 1). Whereas it has been previously noted that the fraction of animal food tends to increase at higher latitudes[25,29], our result suggests that it is mainly the short growing season that explains this gradient, as the effect of latitude itself is non-significant when growing season length is considered. A structural equation model, which considers both direct and indirect effects of the predictors, also confirms the dominant effect of hunting percentage on population density in the observational dataset and supports the link that seasonality influences population density via the hunting percentage (Supplementary Fig. 9 and Supplementary Table 1). Relationships between Φ_{NPP} and other variables, apart from hunting percentage (Fig. 4c), were also examined (Supplementary Fig. 10), showing a significant positive correlation between Φ_{NPP} and growing season length ($r = 0.37$, $P < 0.001$), which, however, becomes non-significant after

controlling for hunting percentage in the partial correlation analysis (Supplementary Table 2).

Discussion

This study built a process-based hunter-gatherer dynamics model, coupled to a global terrestrial biosphere model, to explore the influence of environmental factors on hunter-gatherer population density. The model explicitly simulates microscale processes including daily carbon/energy flows among plants, animals and humans, combined with a dynamic time allocation for hunting and gathering activities with simple assumptions. The emergent macroscopic relationships from the model are well supported by ethnographic observations of contemporary hunter-gatherers, revealing a causal mechanism whereby short growing seasons drive high fractions of meat in the diet, leading to greatly reduced population density per unit NPP largely as a result of trophic inefficiency.

The empirical negative association between hunting fraction and population density has been reported or implied in previous studies[14,30] but it was assumed that population density was the causal factor, rather than vice versa: a higher population density was suggested to lead to less frequent residential moves, more food storage and thus greater dependence on the stationary and higher productive food of plants and coastal resources[14]. Our process-based coupled human–ecosystem model suggests a more parsimonious explanation, given that it reproduces the observed relationships as a straightforward consequence of bioenergetics. Reinforcing mechanisms between demography and diet via cultural factors may still be relevant, as suggested by ref. [14] and by anthropological studies on diet from both ecological/biological and sociocultural perspectives[31]. In particular, food storage and sharing have received much attention, due to their close association with societal characteristics and ability to mitigate food scarcity at daily to seasonal timescales[32–34]. It may be interesting to include food storage and sharing in our model framework in the future to quantitatively explore the interplay between environment, demography, diet and sociocultural aspects.

The integral links between seasonality, diet composition and population density have strong implications for studies that explore ancient human populations. Although seasonal cycles in the availability of different types of food have left traces in fossil teeth of extinct hominins[35] and been detected in the gut microbiome composition of the Hadza foragers in East Africa[36], seasonality has not been included in prior modelling studies[4,6,7,13] that used only annual NPP and/or mean palaeoclimate variables, which would have biased expectations for the spatiotemporal pattern of early human distribution and migration. Furthermore, the lengthening of growing seasons following the last deglaciation, combined with the end-Pleistocene megafaunal extinctions that occurred in different regions at different timing and rates[37], might have driven long-term changes in diet composition towards less meat-dependence. Our results suggest that a shift from meat-dominated to plant-dominated diet could have boosted population much more than implied by NPP changes alone. Given that demography might be at the core of cultural evolution[38], which further shaped human societies[8,39], it is crucial to study the trajectory of past population growth and its drivers, under the changing palaeoclimate, vegetation and animal distributions.

The model developed here represents a new type of computational modelling for ancient human–ecology studies, breaking from a tradition[40] that has mainly included niche (species distribution) models based on statistical methods and without human feedbacks on the environment and agent-based models which resolve individual behaviours and interactions but require very detailed local information that is challenging to assess and have only been applied at a local/community scale[41,42]. By incorporating hunter-gatherers in a realistic, interactive and dynamical global environment, the ESM framework helps to clarify how short growing seasons force humans to rely on meat-rich diets, reducing Φ_{NPP} and thus the population density per unit NPP. Additional factors beyond those resolved in our current model, such as technological transitions[25,43] and long-range migrations, are sure to have played important roles in determining changes in hunter-gatherer population abundance and diet through time. With further development, the approach has the potential to provide more highly resolved pictures of the complex, multifaceted interactions between our ancestors and the Earth system.

Methods

Contemporary hunter-gatherer data. The hunter-gatherer population density and coordinates were acquired from ref. [3], which combined the ethnographic datasets from refs. [1,2,44] (357 datapoints in total). For the diet composition (percentages of hunting, gathering and fishing), we combined the two datasets of subsistence from Kelly[2] and Binford[1,45] (340 datapoints in total), which indicate proportions of food derived from terrestrial animals, terrestrial plants and aquatic resources[1], in terms of weight or calorie[2]. Average of the two datasets were used if a population is present in both sources.

To explore the potential impact of environmental variables on population density and diets, we extracted the values of the following variables from their global maps: annual NPP from the satellite-derived MOD17A3 product[46] (averaged over 2001–2010); fractional coverage of trees and grasses from a satellite-derived vegetation cover product[47]; biodiversity index from ref. [3], which was the average of scaled richness of animals (mammals + birds) and vascular plants; growing season length calculated as the days in a year when daily gross primary production (GPP) exceeds 20% of the maximum daily GPP for each grid cell, wherein the daily GPP was from an upscaled global map based on FLUXNET tower sites[48] (different thresholds were tested but made little difference; for example, growing season lengths defined by thresholds of 10 and 20% are highly correlated, $r = 0.93$). Due to slight differences of the land–sea mask of these global land-only products, a few coastal populations were located in grid cells with a non-valid value; in such a case, the value of the nearest land pixel was used. These potential environmental predictors are used in statistical analyses of the ethnographic data as detailed in Supplementary Discussion 1.

Unlike Tallavaara et al.[3], we did not use the climate-based Miami model to calculate NPP but instead used MODIS NPP because the Miami model was shown to overestimate NPP in the tropics since it only considers annual mean temperature and precipitation and misses important factors such as nutrient limitation in tropical forests[49]. It was argued in ref. [3] that the satellite-based NPP was unfavourable because of the recent human appropriation of NPP. However, we consider it a minor problem here because most of the sites have very small coverages of cropland, according to a satellite product[50] (242 out of the 357 sites have <5% cropland cover; 305 sites <20%).

We calculated the fraction of NPP consumed by hunter-gatherers (Φ_{NPP}), which represents the proportion of total energy available to heterotrophs that flows into hunter-gatherers, as follows: per capita daily energy consumption, averaged over eight different groups[2], is 2,480 kcal ind.$^{-1}$ d^{-1}, which equals to 174 kgC ind.$^{-1}$ yr^{-1}, using the conversion coefficients of 9.8 MJ per kg of dry mass (kgDM^{-1}) (see the text below equation (4)) and 0.45 gC gDM^{-1}. This same value is multiplied by population density and divided by NPP to derive Φ_{NPP} for each site.

A potential systematic bias in the ethnographic diet composition data is worth attention. In this study, we regard the recorded hunting fractions as representing meat fractions of the diet. However, the hunting fractions are likely to underestimate the true consumption of animals due to the fact that early observers had devalued women's contribution in meat provision, including small animals, eggs and insects. Such contributions had been often categorized as 'gathering', or simply ignored, as the focus of 'hunting' had been on relatively large, mobile prey. This bias could be large for groups in arid regions, for example, the Western Desert in Australia[51,52], for which the recorded hunting percentage is about 30% while the true meat fractions are up to 80% when women's contribution to hunting is included[51]. The bias appears to be lower for groups in the tropics such as Amazon Basin and Congo Basin[53], where recent field observations show <10% of total hunted food from women[53]. Unfortunately, revisiting and verifying the secondary data on diet composition is difficult due to the disappearance of the foraging lifestyles for most of the recorded hunter-gatherer groups. We therefore conducted a sensitivity test to see how the observed negative relationship between Φ_{NPP} and hunting fraction (Fig. 4c) might be influenced by expected uncertainties and biases in the ethnographic dietary records. As detailed in Supplementary Discussion 1, we found that the relationship between Φ_{NPP} and hunting fraction is robust to the expected biases, with only a minor impact on the slope of the correlation over the most probable range of bias.

Description of the process-based hunter-gatherer dynamics model. *Model overview.* We designed the hunter-gatherer dynamics model, FORGE, in the framework of Earth system models. It is coupled to the ORCHIDEE (Organizing

Carbon and Hydrology In Dynamic Ecosystems) terrestrial biosphere model[54], which is the land component of the IPSL (Institut Pierre Simon Laplace) ESM. ORCHIDEE simulates the energy and water balance, vegetation dynamics and carbon cycle of land ecosystems. Inputs for ORCHIDEE include meteorological variables (air temperature, precipitation, incoming short and long wave radiation, wind speed, air humidity and air pressure), atmospheric CO_2 concentration, land cover, topography and soil texture maps. Spatial resolution and domain of each simulation are customized depending on the inputted climate forcing. In the model, each grid cell is occupied by a suite of plant functional types (PFTs), with their fractional covers adding up to one. ORCHIDEE has recently incorporated a module of large mammalian herbivores that simulates animal population density driven by vegetation and climate[17]. The main revision of the herbivore module compared to ref. [17] is the inclusion of browsers (herbivores that eat woody plants) whereas the previous version only calculated grazers. The same parameterizations are used for browsers as for grazers, except that browsers feed on the leaf and fruit compartments of tree PFTs, assuming 10% of this biomass is reachable to browsers. The summation of grazer and browser density in each grid cell provides the potential animal food density for humans.

The new FORGE model (Fig. 2) couples hunter-gatherers with vegetation and herbivores in each grid cell via daily foraging activities and resultant carbon/energy flows, which then updates an energetic reserve (body fat) that determines birth rate and mortality rate of human populations. The human foraging activities are formulated on the basis of a time allocation scheme. The feedback of human hunting on herbivore dynamics is taken into account, while the impact of humans on vegetation growth is neglected in the current model but the model infrastructure leaves room for future developments regarding human-induced environmental changes (for example, changes in land cover and fire regimes) and subsequent impacts on the ecosystems. Major simplifications of FORGE include that: (1) only an average human (body weight = 50 kg ind.$^{-1}$) is represented; (2) fishing is not implemented in the current land-only model, leading to a potential underestimation in population density of the groups for which marine resources provide much food, mostly in coastal regions (Supplementary Fig. 1); (3) human migration[55] across grid cells is not accounted for, although the fact that the ethnographically recorded average migration distance per move and the total distance moved between camps in a year are about 27 and 280 km, respectively[1], means that most hunter-gatherers would not move over more than the dimensions of one grid cell (on the order of 10^4 km^2 each) in an annual cycle; and (4) the lack of representation of small animals in the model, including birds, reptiles, insects and small mammals (<5–10 kg ind.$^{-1}$), could lead to underestimations in available animal food and meat fraction of the diet, which coincides with the potential systematic underestimations in the ethnographic hunting fraction data mentioned above. Detailed formulations of FORGE are described below.

Daily intake. The model considers two types of subsistence activity: hunting and gathering. The contribution of each activity to the diet depends on the abundance of animal biomass and edible vegetation biomass, the time spent in hunting and gathering, as well as the technology-dependent efficiency of both activities:

$$\begin{aligned} I_V &= B_V\, t_g\, e_g\, a \\ I_A &= B_A\, t_h\, e_h\, a \end{aligned} \tag{1}$$

where I_V and I_A are daily dry matter intake of vegetation and meat (kgDM d^{-1} ind.$^{-1}$); B_V and B_A are biomass density of edible vegetation and animals (kgDM m^{-2}); t_g and t_h are the time allocated to gathering and hunting (h d^{-1}); a is the searching area per person hour, fixed at 4,000 m^2 h^{-1} ind.$^{-1}$; e_g and e_h are the efficiencies of gathering and hunting, representing the fraction of the corresponding biomass that is acquired when hunter-gatherers pass the searched area.

In a linear form this equation would imply that the food resources and foragers are both uniformly distributed within each grid cell and foragers encounter them randomly. In reality, excursions are undertaken from localized camps, different food items are distributed in patches and foragers know how to target the higher energy-return items first[2]. To partly account for these aspects of subgrid heterogeneity, we assume e_g and e_h to decrease as B_v and B_a decrease relative to human density, capturing the increasing difficulty of foraging as the best resources are sequentially depleted. We model this with an asymptotic function:

$$\begin{aligned} e_g &= e_{max}\frac{B_V}{B_V + c\,B_H} \\ e_h &= e_{max}\frac{B_A}{B_A + c\,B_H} \end{aligned} \tag{2}$$

where B_H is human biomass density (kg m^{-2}), equal to P_H (population density which is prognostically simulated in the model; equation(11)) multiplied by mean body weight (W_H, 50 kg ind.$^{-1}$); e_{max} is the maximum fraction of the edible plant/animal biomass that can be acquired when hunter-gatherers pass the searched area, fixed at 1 and tested in a sensitivity analysis (below); c determines the patch depletion rate; the value of c is fixed at 100 and is tested in the sensitivity analysis. Notably, the inclusion of equation (2) produces a dynamic similar to that found in ecological studies of per capita prey consumption by wild predators, which often decreases with predator density for a given prey density[56].

Energy expenditure and energetic reserve. The per capita daily energy expenditure E (MJ d^{-1} ind.$^{-1}$) is calculated as:

$$E = E_c + E_g\, t_g + E_h\, t_h \tag{3}$$

where E_c is the energy expenditure excluding those spent during foraging, fixed as 8.37 MJ d^{-1} ind.$^{-1}$ (that is, 2,000 kcal d^{-1} ind.$^{-1}$); E_g and E_h are the energy spent per hour gathering or hunting, fixed as 1.25 MJ h^{-1} ind.$^{-1}$ (according to ref. [57]) for both parameters in the model.

On the basis of daily food intake and energy expenditure, per capita energetic reserve (mainly in fat cells) is updated daily as below. This is the key variable that indicates health condition and is used to calculate birth rate and mortality rate (below).

$$\begin{aligned} \frac{dF}{dt} &= \frac{I-E}{m} \\ I &= m_V\, I_V + m_A\, I_A \end{aligned} \tag{4}$$

where F (kg ind.$^{-1}$) is per capita energetic reserve; m (MJ kg^{-1}) is the conversion coefficient between energy and fat mass, set to 39.3 if $I < E$ (catabolism) or 54.6 if $I > E$ (anabolism) (ref. [58]). The gross energy value of plants and animals is around 3,800–4,800 for different plants (~5,000 for seeds) and 4,400–5,600 for different animal taxa (ref. [59]; in the unit kcal kgDM^{-1}). We thus assume the same value for both food types for simplicity. Further, considering the ~30% energy loss in excreta and that the metabolizable energy content is less than the gross energy value of food, we finally set m_V and m_A to 9.8 MJ kgDM^{-1}. It should be noted that the energy density of a mammal's carcass depends on its fat content[22]; thus a fixed m_A value in the current model is a simplification and does not account for variations across species and over time.

There is an upper limit of F (F_{max}), assumed to be 30% of body weight, that is 15 kg ind.$^{-1}$ in the model. Accordingly, whenever F is about to exceed F_{max}, daily intake will be reduced so that F stays at F_{max}.

Time allocation. In the current model, we only simulate the time spent in foraging and leave all other activities such as childcare, domestic maintenance and socializing to an aggregate 'other' category. The hunting, gathering and total foraging time ($t_f = t_h + t_g$) are updated every day in the following two steps. First, t_f increases or decreases by 1 h d^{-1}, depending on the changes in the energetic reserve F during the previous day:

$$\begin{aligned} t_f(t) &= \begin{cases} t_f(t-1) - 1, & \text{if} \Delta F > 0 \text{ and } F(t) > 0.5F_{max} \\ t_f(t-1) + 1, & \text{else} \end{cases} \\ t_f &\in [t_{f,min}, t_{f,max}] \end{aligned} \tag{5}$$

t_h and t_g are then changed proportionately. Such reduction of foraging time when humans have eaten plenty of food in the previous day could represent idle relaxation, a phenomenon widely observed in many animals[60] as well as hunter-gatherers[61]. An upper limit on foraging time would also be driven by the need to do the other essential activities not modelled here. Foraging times reported for dozens of hunter-gatherer groups, averaged between males and females, range between 0.8 and 6.8 h d^{-1} (refs. [2,18,19]). We therefore set $t_{f,min} = 0.5$ and $t_{f,max} = 8$ h d^{-1}.

Second, the allocation between hunting and gathering depends on the relative energy benefit of the two activities, as well as a craving for meat, parameterized as an exponential decay function of meat proportion in the diet of the previous day:

$$\begin{aligned} th_{frac} &= \frac{benefit_h}{benefit_h + benefit_g} C_{meat} \\ f_{meat} &= \frac{I_A}{I_A + I_V} \\ C_{meat} &= e^{-q(f_{meat}-1)} \\ benefit_h &= B_A\, e_h \\ benefit_g &= B_V\, e_g \\ th_{frac} &\in [0.05, 0.95] \end{aligned} \tag{6}$$

where th_{frac} is the fraction of t_f allocated to hunting. The additional meat-craving term, C_{meat}, is introduced to represent that hunter-gatherers generally have a preference for meat, which may reflect nutritional needs (for example, fat and essential amino acids)[62] as well as cultural importance[2]. The parameter q is fixed at 2.5 but also tested (Supplementary Table 3). In cases when f_{meat} falls below 10% (the minimum observed hunting + fishing fraction), th_{frac} is set to 0.95. Variables t_h and t_g are then calculated as $t_f \times th_{frac}$ and $t_f \times (1 - th_{frac})$, respectively.

This time allocation scheme is highly simplified. It does not consider, for example, seasonal variations of other necessary activities such as providing shelter, extreme weather that makes foraging activities risky or unworthy (for example,

the Hiwi in tropical savannah do not forage during the middle of the day to avoid heat[27]) and additional social/cultural factors. Further improvements and tests of the scheme are possible in the future, given more observational data on human time allocation dynamics. Yet, it provides an unprecedented approach to include the fundamental limit of time on the ability to capture existing biomass.

Updating food resources. Not all vegetation and herbivore biomass are edible or accessible to humans. We denote the edible and/or accessible fraction of vegetation and herbivores as Φ_V and Φ_A, respectively, which are assumed to be fixed parameters in the current model over the globe ($\Phi_V = 0.015$, $\Phi_V = 0.1$; sensitivity tests below). This is a simplification; for example, many fruits in tropical forests grow high in the canopy, making them harder to reach than is the case in short-vegetation biomes[2]. Unfortunately, robust estimates of the edible/accessible fraction for major biomes worldwide are unavailable and, therefore, we do not vary Φ_V and Φ_A between grid cells in the current model, to avoid arbitrarily introducing spatial relationships of human density versus NPP. Apart from fruits, hunter-gatherers can also eat roots and tubers, which are from the belowground primary production of some herbaceous plants. We thus also include part of the belowground grass NPP as potential food sources.

The B_V (biomass density of edible vegetation) is updated on a daily time step:

$$\begin{aligned} \frac{dB_V}{dt} &= \Phi_V(f_{fruit}\mathrm{NPP} + f_{below}\mathrm{NPP}_{grass}) - \lambda B_V - I_V P_H \\ f_{below} &= \frac{88.3 - 0.0534\,\mathrm{MAP}}{100} \end{aligned} \quad (7)$$

Where λ (d^{-1}) is the daily turnover rate of the edible vegetation biomass; f_{fruit} is the fraction of NPP (including both tree and grass) allocated to fruits, set to 6.5% in the current model according to a synthesis[63] of fruit fall observations across tropical and temperate forests; f_{below} is the fraction of grass NPP allocated belowground, calculated as a function of mean annual precipitation (MAP, mm yr^{-1}) following the empirical equation from ref. [64], which captures the higher belowground allocations in dryer ecosystems. The lower limit of f_{below} is set to 20%. The inputted NPP and λ are either from ORCHIDEE outputs or from observation-derived values (section Model setup describes the different runs).

The herbivore dynamics module is coupled once per year with the human dynamics module. Detailed descriptions of the herbivore module can be found in ref. [17]. In summary, herbivore population density ($P_{A,tot}$, ind. km^{-2}) is updated on a yearly time step using a logistic equation (equation 8 in ref. [17]). The herbivore birth and mortality rates depend on an animal fat reserve pool (kg ind.$^{-1}$) that is updated daily according to their energy intake through grazing or browsing.

Within the human module, B_A is updated on a daily time step:

$$\frac{dB_A}{dt} = -I_A P_H \quad (8)$$

At the end of each year, the accumulated number of hunted animals $\left(\frac{\sum I_A P_H}{W_A \times 0.28}\right)$ is subtracted from the herbivore population density $P_{A,tot}$. The decreased $P_{A,tot}$ is passed to the herbivore module to calculate a new $P_{A,tot}$ for the next year. B_A is then updated and used in the human module for the new year:

$$B_A = \Phi_A P_{A,tot} W_A \times 0.28 \quad (9)$$

where W_A is the mean body weight of herbivores, set to 180 kg ind.$^{-1}$ in the current model; 0.28 is the conversion between live weight and dry mass after excluding water and bones.

Note that the herbivore population dynamics is also affected by seasonality, with relatively higher animal starvation mortalities in regions with longer winters/dry seasons[17]. However, temporally, simulated meat density is relatively stable throughout the year in the model (Fig. 5) because the animal population density is updated only once per year. The annual update is justified by the fact that the animals represented have lifespans of ~25 yr (ref. [17]), so that seasonal fluctuations in population numbers are strongly damped. Unlike humans, herbivores can feed on plant litter (dead grasses and fallen leaves/fruits in the model) to live through non-growing seasons, providing vital food for hunter-gatherers to survive the long winters/dry seasons in the model.

It should be emphasized that the modelled feedbacks of human foraging are very different for vegetation and animal density. Gathering is assumed to have negligible impacts on primary productivity, since the B_v that is harvested represents the edible part of plants, which generally do not contribute to plant growth and for which harvesting can even aid in reproduction (for example, through the spreading of seeds[65]). In contrast, hunting can directly reduce the annual production of herbivores by reducing $P_{A,tot}$. However this effect would be small at low rates of hunting, for which competition among herbivores places the limit on $P_{A,tot}$.

Human population dynamics. The population birth rate (r_{birth}, yr^{-1}) is assumed to depend on the average body condition, represented by the daily-varying energetic reserve F. Thus, r_{birth} is calculated every day and averaged over the year to be used in equation (11),

$$r_{birth} = \frac{r_a}{1 + e^{-r_b\left(\frac{F}{F_{max}} - r_c\right)}} \quad (10)$$

where $r_a = 0.1$, $r_b = 15$ and $r_c = 0.5$. This sigmoidal function is similar to the equation used to calculate herbivore birth rate[17], with the parameters modified so as to give a maximum birth rate of 10%, close to the recorded highest crude birth rate during the past two centuries (~6%, ref. [66]) (sensitivity tests of the three parameters are below).

For mortality, we consider two processes. First, a background mortality rate (M_b) which is the inverse of lifespan, fixed as $\frac{1}{80} = 0.0125\,yr^{-1}$. Second, starvation-induced mortality (M_s, yr^{-1}), caused by the exhaustion of body energy storage as represented by the complete depletion of fat reserves. The M_s is calculated using a similar method as in the herbivore module[17]. Namely, we assume a normal distribution of body fat within the population, with a mean $\mu = F$ and a standard deviation $\sigma = 0.125 F_{max}$; the probability that fat mass falls below 0 is taken as the value of M_s. Similar to r_{birth}, M_s is also calculated every day and averaged over the year.

Finally, the annual dynamics of the human population density are calculated as:

$$\frac{dP_H}{dt} = r_{birth} P_H - (M_s + M_b) P_H \quad (11)$$

where P_H (ind. km^{-2}) is the human population density for each grid cell. The P_H is initialized as $P_0 = 10^{-3}$ ind. km^{-2}, a lower value than the minimum density ever recorded (0.002 ind. km^{-2}; ref. [1,2]). Whenever P_H falls below P_0, P_H is reset to P_0.

Once each year, the reproduction energy cost (313 kcal d^{-1} or 478 MJ for a year, according to ref. [67]) is subtracted from the energetic reserve F to account for the energy input to birth:

$$\Delta F = -\frac{478\, r_{birth}}{m} \quad (12)$$

Model setup. To derive the input variables for FORGE, we firstly ran ORCHIDEE for the globe at 2° spatial resolution and for 200 yr as a spin-up to reach the equilibrium of vegetation production and biomass under present-day climate conditions. The climate forcing was the CRU-NCEP reanalysis dataset[68], repeating the years 2001–2010. The atmospheric CO_2 concentration was fixed at 380 ppm (the average level during 2001–2010). For the land cover, although ORCHIDEE can simulate vegetation distributions equilibrated under the given climate conditions, we instead prescribed an observation-based PFT map to reduce the bias of ORCHIDEE outputs that would propagate to the FORGE model. This PFT map was based on ESA CCI Land Cover map v.2.0.7b for 2010, which was further merged with the LUH2 dataset to generate a pre-industrial PFT map (year 850) with minimal crop coverages. Detailed descriptions of the PFT map can be found at https://orchidas.lsce.ipsl.fr/dev/lccci/.

The last 10 years' outputs from ORCHIDEE are used to provide the inputs to FORGE. These include the inputs required by the herbivore module: fractional cover of PFTs (aggregated into three types: grass, tree and bare ground), carbon influx rates (that is, NPP allocated to the edible plant tissues and influx to the edible litter pool) and decay rates of the edible pools and annual mean temperature; as well as inputs required by the human module: NPP, decay rate of the fruit compartment and annual precipitation (used in equation (7)). The input variables are at a daily time step. FORGE was then run for 300 yr to reach the equilibrium of population density of both herbivores and hunter-gatherers. The last 50 yr were averaged and presented as the results.

Supplementary Fig. 11 shows the ORCHIDEE-simulated NPP, in comparison with MODIS NPP. ORCHIDEE can reproduce the overall pattern of the satellite-derived NPP, with a reasonable agreement with MODIS NPP at the sites (Pearson correlation coefficient $r = 0.67$). However, ORCHIDEE underestimated NPP in tropical forests and arid ecosystems including some classical hunter-gatherer areas such as the Great Basin in North America, Kalahari in southern Africa and interior Australia (Supplementary Fig. 11). The underestimation of annual NPP in the dry regions is partly due to an underestimation of growing season length by ORCHIDEE (Supplementary Fig. 12).

To test the impact of the bias of ORCHIDEE-simulated NPP and to minimize this bias that would propagate to the FORGE-simulated hunter-gatherer densities, we conducted three sets of simulations, with different input files while identical FORGE model:

S0: inputs to FORGE are directly from ORCHIDEE outputs;
S1: compared to S0, the daily NPP is multiplied by a scaling factor so that the annual NPP (average for 2001–2010) equals to MODIS NPP for each grid cell;
S2: compared to S0, the daily NPP is replaced by the observation-based values; that is, annual MODIS NPP interpolated into daily values according to an observation-derived daily GPP product[48]. Note that the herbivore module in FORGE separates grazers feeding on grass NPP and browsers feeding on tree NPP and here we assume the same NPP values (per unit PFT area) for tree and grass PFTs in the same grid cell. Besides, the ORCHIDEE-simulated daily decay rates of edible plant tissues (λ) are replaced by a constant of 0.01 d^{-1} during growing season (when $NPP_{daily} > NPP_{daily,max}$) and 0.05 d^{-1} during non-growing season (when $NPP_{daily} <= NPP_{daily,max}$), to avoid an inconsistent timing of senescence (a period of high decay rates of leaves and fruits) with the observed seasonality in NPP. The λ values are chosen so that the integrated annual decay rates are generally comparable to those simulated by ORCHIDEE (used in S0 and S1).

Modelled population densities and their relationships between NPP and meat fraction of the diet from the S0 and S1 runs are shown in Supplementary Figs. 13 and 14. Among S0, S1 and S2, the emergent relationships between population density and NPP, and Φ_{NPP} and meat fraction, are similar (Supplementary Fig. 14), except for a steeper slope of log(population density) versus NPP in S0 due to the lack of datapoints under the high end of NPP (as ORCHIDEE underestimates NPP in tropical forests; Supplementary Fig. 11). Regarding the global patterns of population density (Supplementary Fig. 13), however, both S0 and S1 predict an unrealistic absence of hunter-gatherers in many arid ecosystems, including those in western Plains in North America, Kalahari and interior Australia, the classical hunter-gatherer territories. These regions are populated in the S2 results (Fig. 3a). The difference between S1 and S2 (for which the annual total NPP in the inputs are identical) therefore indicates the critical role of a substantially long growing season length in sustaining hunter-gatherers in the less productive ecosystems. Considering a prevailing underestimation in growing season length for the arid ecosystems in state-of-the-art terrestrial biosphere models (Supplementary Fig. 15), our results highlight the need for a more realistic simulation of plant phenology to improve the simulation of contemporary and ancient hunter-gatherers. Unless otherwise specified, the model results shown are from the S2 experiment.

Sensitivity tests of parameters. We consider several parameters in FORGE, listed in Supplementary Table 3, to be highly uncertain. We therefore conducted sensitivity tests using Sobol's method[69] (a variance-based sensitivity analysis), which decomposes the variance of model output into fractions that can be attributed to different inputs. Sobol's method has the advantage of measuring sensitivity across the whole input space, as well as accounting for nonlinearity and parameter interactions, so that the total-order index (S_T) indicates the importance of each parameter considering both its main effect (first-order sensitivity index, S_1) and the contribution of its interaction with other parameters.

Sobol's method requires thousands of runs, which is computationally expensive for global experiments. We thus carried out the tests at two sites with contrasting characteristics. First, a temperate forest with a long growing season and a low hunting fraction in the diet at 42° N, 123° W. Second, a boreal forest with a short growing season and a high hunting fraction at 56° N, 69° W (Supplementary Fig. 16). For each site, we conducted 9,000 runs in which the parameters were sampled within their ranges listed in Supplementary Table 3, using Saltelli's sampling scheme which is more efficient than random sampling. Supplementary Fig. 17 shows how the varied parameter values affect the corresponding equations. All the sensitivity tests were done using the Python package 'SALib' (https://salib.readthedocs.io/en/latest/index.html).

The resulting S_T and S_1 (Supplementary Fig. 18) indicate different sensitivities to the parameters between the two sites. For the hunting-dominated site, population density is most sensitive to Φ_A, followed by e_{max} and c, whereas for the gathering-dominated site, population density is sensitive to the four parameters Φ_V, Φ_A, e_{max} and c. The three parameters used to calculate birth rate make negligible contributions to the variance in modelled population. Indeed, birth rate impacts the time it takes to reach equilibrium population under a given set of environmental conditions but has a negligible effect on the equilibrium value itself. Nor is the population density sensitive to the parameter q, which determines the meat-craving response.

Supplementary Fig. 19 further shows the quantitative response of model results to the parameters. As expected, a higher Φ_V (or Φ_A) value increases population density at the gathering-dominated (or hunting-dominated) site, while a higher c value decreases the population at both sites. A higher e_{max} value increases population density at both sites but the beneficial effect diminishes at high population densities for the hunting-dominated site, probably a result of overhunting. Meat fraction in the diet is mainly determined by the relative values of Φ_V and Φ_A (Supplementary Fig. 18). Compared to population density and meat fraction, foraging time is relatively more equally sensitive to all the tested parameters (Supplementary Fig. 18) but its results in the 9,000 runs are relatively centralized across the tested parameter space for both sites (Supplementary Fig. 19).

For the standard configuration, we set $\Phi_V = 0.015$, $\Phi_A = 0.1$, $e_{max} = 1$ and $c = 200$ so as to match the average value of population density and meat fraction across the sites. Note that changing these globally-constant parameter values increases or decreases population everywhere but has minor impacts on the modelled relationships with environmental variables (Supplementary Fig. 20).

Reporting Summary. Further information on research design is available in the Nature Research Reporting Summary linked to this article.

Data availability

The contemporary hunter-gatherer data and environmental variables used in the analysis are available in the Supplementary Data.

Code availability

Source code (in Python) of the FORGE model and its output files (in NetCDF format) for this study, including the three sets of global simulations (S0, S1, S2), are provided in Supplementary Software. The corresponding input files for the FORGE model are available at https://doi.org/10.6084/m9.figshare.14995320.v2.

Received: 23 September 2020; Accepted: 4 August 2021;
Published online: 9 September 2021

References

1. Binford, L. R. *Constructing Frames of Reference: An Analytical Method for Archaeological Theory Building Using Hunter-Gatherer and Environmental Data Sets* (Univ. of California Press, 2001).
2. Kelly, R. L. *The Lifeways of Hunter-Gatherers: The Foraging Spectrum* (Cambridge Univ. Press, 2013).
3. Tallavaara, M., Eronen, J. T. & Luoto, M. Productivity, biodiversity, and pathogens influence the global hunter-gatherer population density. *Proc. Natl Acad. Sci. USA* **115**, 1232–1237 (2018).
4. Eriksson, A. et al. Late Pleistocene climate change and the global expansion of anatomically modern humans. *Proc. Natl Acad. Sci. USA* **109**, 16089–16094 (2012).
5. Gurven, M. D. & Davison, R. J. Periodic catastrophes over human evolutionary history are necessary to explain the forager population paradox. *Proc. Natl Acad. Sci. USA* https://doi.org/10.1073/pnas.1902406116 (2019).
6. Tallavaara, M., Luoto, M., Korhonen, N., Järvinen, H. & Seppä, H. Human population dynamics in Europe over the Last Glacial Maximum. *Proc. Natl Acad. Sci. USA* **112**, 8232–8237 (2015).
7. Bradshaw, C. J. A. et al. Minimum founding populations for the first peopling of Sahul. *Nat. Ecol. Evol.* **3**, 1057–1063 (2019).
8. Kavanagh, P. H. et al. Hindcasting global population densities reveals forces enabling the origin of agriculture. *Nat. Hum. Behav.* **2**, 478–484 (2018).
9. Porter, C. C. & Marlowe, F. W. How marginal are forager habitats? *J. Archaeol. Sci.* **34**, 59–68 (2007).
10. Reyes-García, V. & Pyhälä, A. *Hunter-Gatherers in a Changing World* (Springer International Publishing, 2017).
11. Lee, R. B. & Daly, R. *The Cambridge Encyclopedia of Hunters and Gatherers* (Cambridge Univ. Press, 1999).
12. Kitanishi, K. Seasonal changes in the subsistence activities and food intake of the Aka hunter-gatherers in northeastern Congo. *Afr. Study Monogr.* **16**, 73–118 (1995).
13. Timmermann, A. & Friedrich, T. Late Pleistocene climate drivers of early human migration. *Nature* **538**, 92–95 (2016).
14. Keeley, L. H. Hunter-gatherer economic complexity and 'population pressure': a cross-cultural analysis. *J. Anthropol. Archaeol.* **7**, 373–411 (1988).
15. Fisher, J. B., Huntzinger, D. N., Schwalm, C. R. & Sitch, S. Modeling the terrestrial biosphere. *Annu. Rev. Environ. Resour.* **39**, 91–123 (2014).
16. Pachzelt, A., Forrest, M., Rammig, A., Higgins, S. I. & Hickler, T. Potential impact of large ungulate grazers on African vegetation, carbon storage and fire regimes. *Glob. Ecol. Biogeogr.* **24**, 991–1002 (2015).
17. Zhu, D. et al. The large mean body size of mammalian herbivores explains the productivity paradox during the Last Glacial Maximum. *Nat. Ecol. Evol.* **2**, 640–649 (2018).
18. Dyble, M., Thorley, J., Page, A. E., Smith, D. & Migliano, A. B. Engagement in agricultural work is associated with reduced leisure time among Agta hunter-gatherers. *Nat. Hum. Behav.* **3**, 792–796 (2019).
19. Hill, K., Kaplan, H., Hawkes, K. & Hurtado, A. M. Men's time allocation to subsistence work among the Ache of eastern Paraguay. *Hum. Ecol.* **13**, 29–47 (1985).
20. Hill, K., Hawkes, K., Hurtado, M. & Kaplan, H. Seasonal variance in the diet of Ache hunter-gatherers in eastern Paraguay. *Hum. Ecol.* **12**, 101–135 (1984).
21. Marlowe, F. W. et al. Honey, Hadza, hunter-gatherers, and human evolution. *J. Hum. Evol.* **71**, 119–128 (2014).
22. Cordain, L. et al. Plant–animal subsistence ratios and macronutrient energy estimations in worldwide hunter-gatherer diets. *Am. J. Clin. Nutr.* **71**, 682–692 (2000).
23. Gurven, M. & Kaplan, H. Longevity among hunter-gatherers: a cross-cultural examination. *Popul. Dev. Rev.* **33**, 321–365 (2007).
24. Klein Goldewijk, K., Beusen, A. & Janssen, P. Long-term dynamic modeling of global population and built-up area in a spatially explicit way: HYDE 3.1. *Holocene* **20**, 565–573 (2010).
25. Marlowe, F. W. Hunter-gatherers and human evolution. *Evol. Anthropol.* **14**, 54–67 (2005).
26. Burger, J. R. & Fristoe, T. S. Hunter-gatherer populations inform modern ecology. *Proc. Natl Acad. Sci. USA* **115**, 1137–1139 (2018).
27. Hurtado, A. M. & Hill, K. R. Seasonality in a foraging society: variation in diet, work effort, fertility, and sexual division of labor among the Hiwi of Venezuela. *J. Anthropol. Res.* **46**, 293–346 (1990).
28. Wilmsen, E. N. Studies in diet, nutrition, and fertility among a group of Kalahari Bushmen in Botswana. *Soc. Sci. Inf.* **21**, 95–125 (1982).
29. Lee, R. B. in *Man the Hunter* (eds. Lee, R. B. & DeVore, I.) 30–48 (Aldine de Gruyter, 1968).

30. Hamilton, M. J., Milne, B. T., Walker, R. S. & Brown, J. H. Nonlinear scaling of space use in human hunter-gatherers. *Proc. Natl Acad. Sci. USA* **104**, 4765–4769 (2007).
31. Messer, E. Anthropological perspectives on diet. *Annu. Rev. Anthropol.* **13**, 205–249 (1984).
32. Testart, A. et al. The significance of food storage among hunter-gatherers: residence patterns, population densities, and social Inequalities [and Comments and Reply]. *Curr. Anthropol.* **23**, 523–537 (1982).
33. Winterhalder, B. Diet choice, risk, and food sharing in a stochastic environment. *J. Anthropol. Archaeol.* **5**, 369–392 (1986).
34. Kelly, R. L., Pelton, S. R. & Robinson, E. in *Towards a Broader View of Hunter-Gatherer Sharing* (eds Lavi, N. & Friesem, D. E.) Ch. 10 (McDonald Institute for Archaeological Research, 2019).
35. Joannes-Boyau, R. et al. Elemental signatures of *Australopithecus africanus* teeth reveal seasonal dietary stress. *Nature* **572**, 112–115 (2019).
36. Smits, S. A. et al. Seasonal cycling in the gut microbiome of the Hadza hunter-gatherers of Tanzania. *Science* **357**, 802–806 (2017).
37. Barnosky, A. D. Assessing the causes of Late Pleistocene extinctions on the continents. *Science* **306**, 70–75 (2004).
38. Henrich, J. Demography and cultural evolution: how adaptive cultural processes can produce maladaptive losses—the Tasmanian case. *Am. Antiq.* **69**, 197–214 (2004).
39. Powell, A., Shennan, S. & Thomas, M. G. Late Pleistocene demography and the appearance of modern human behavior. *Science* **324**, 1298–1301 (2009).
40. D'Alpoim Guedes, J. A., Crabtree, S. A., Bocinsky, R. K. & Kohler, T. A. Twenty-first century approaches to ancient problems: climate and society. *Proc. Natl Acad. Sci. USA* **113**, 14483–14491 (2016).
41. Cegielski, W. H. & Rogers, J. D. Rethinking the role of Agent-based modeling in archaeology. *J. Anthropol. Archaeol.* **41**, 283–298 (2016).
42. Axtell, R. L. et al. Population growth and collapse in a multiagent model of the Kayenta Anasazi in long house valley. *Proc. Natl Acad. Sci. USA* **99**, 7275–7279 (2002).
43. Hayden, B. Research and development in the stone age: technological transitions among hunter-gatherers. *Curr. Anthropol.* **22**, 519–548 (1981).
44. Itkonen, T. I. *Suomen Lappalaiset Vuoteen 1945. Ensimmäinen Osa* (WSOY, 1848).
45. Kirby, K. R. et al. D-PLACE: a global database of cultural, linguistic and environmental diversity. *PLoS ONE* **11**, e0158391 (2016).
46. *MODIS NPP* (MOD17A3) (NTSG, accessed 12 March 2015); http://files.ntsg.umt.edu/data/NTSG_Products/MOD17/
47. Defries, R.S. et al. *ISLSCP II Continuous Fields of Vegetation Cover, 1992–1993* (ORNL DAAC, 2009); https://doi.org/10.3334/ORNLDAAC/931
48. Bodesheim, P., Jung, M., Gans, F., Mahecha, M. D. & Reichstein, M. Upscaled diurnal cycles of land–atmosphere fluxes: a new global half-hourly data product. *Earth Syst. Sci. Data* **10**, 1327–1365 (2018).
49. Šímová, I. & Storch, D. The enigma of terrestrial primary productivity: measurements, models, scales and the diversity–productivity relationship. *Ecography* **40**, 239–252 (2017).
50. Bontemps, S. et al. Consistent global land cover maps for climate modelling communities: current achievements of The ESA Land Cover CCI. In *Proc. ESA Living Planet Symposium 2013* (ESA, 2013).
51. Bliege Bird, R. & Bird, D. W. Why women hunt—risk and contemporary foraging in a western desert aboriginal community. *Curr. Anthropol.* **49**, 655–693 (2008).
52. Bliege Bird, R., Codding, B. F. & Bird, D. W. What explains differences in men's and women's production? *Hum. Nat.* **20**, 105–129 (2009).
53. Reyes-García, V., Díaz-Reviriego, I., Duda, R., Fernández-Llamazares, Á. & Gallois, S. 'Hunting otherwise'—women's hunting in two contemporary forager-horticulturalist societies. *Hum. Nat.* **31**, 203–221 (2020).
54. Krinner, G. et al. A dynamic global vegetation model for studies of the coupled atmosphere-biosphere system. *Global Biogeochem. Cycles* **19**, GB1015 (2005).
55. Hamilton, M. J., Lobo, J., Rupley, E., Youn, H. & West, G. B. The ecological and evolutionary energetics of hunter-gatherer residential mobility. *Evol. Anthropol.* **25**, 124–132 (2016).
56. Abrams, P. A. & Ginzburg, L. R. The nature of predation: prey dependent, ratio dependent or neither? *Trends Ecol. Evol.* **15**, 337–341 (2000).
57. Winterhalder, B., Baillargeon, W., Cappelletto, F., Randolph Daniel, I. & Prescott, C. The population ecology of hunter-gatherers and their prey. *J. Anthropol. Archaeol.* **7**, 289–328 (1988).
58. Illius, A. W. & O'Connor, T. G. Resource heterogeneity and ungulate population dynamics. *Oikos* **89**, 283–294 (2000).
59. Golley, F. B. Energy values of ecological materials. *Ecology* **42**, 581–584 (1961).
60. Herbers, J. M. Time resources and laziness in animals. *Oecologia* **49**, 252–262 (1981).
61. Raichlen, D. A. et al. Sitting, squatting, and the evolutionary biology of human inactivity. *Proc. Natl Acad. Sci. USA* https://doi.org/10.1073/pnas.1911868117 (2020).
62. Abrams, H., Jr. in *Food and Evolution* (eds Harris, M. & Ross, E.) 207–223 (Temple Univ. Press, 1987).
63. Hanya, G. & Aiba, S. Fruit fall in tropical and temperate forests: implications for frugivore diversity. *Ecol. Res.* **25**, 1081–1090 (2010).
64. Gherardi, L. A. & Sala, O. E. Global patterns and climatic controls of belowground net carbon fixation. *Proc. Natl Acad. Sci. USA* https://doi.org/10.1073/pnas.2006715117 (2020).
65. van Zonneveld, M. et al. Human diets drive range expansion of megafauna-dispersed fruit species. *Proc. Natl Acad. Sci. USA* **115**, 3326–3331 (2018).
66. Max R., Hannah R. & Esteban Ortiz-Ospina *World Population Growth* (GCDL, 2020); https://ourworldindata.org/world-population-growth
67. Pontzer, H. et al. Metabolic acceleration and the evolution of human brain size and life history. *Nature* **533**, 390 (2016).
68. Viovy, N. *CRUNCEP Version 7—Atmospheric Forcing Data for the Community Land Model* (Research Data Archive at the National Center for Atmospheric Research, Computational and Information Systems Laboratory, 2018); https://doi.org/10.5065/PZ8F-F017
69. Sobol, I. Global sensitivity indices for nonlinear mathematical models and their Monte Carlo estimates. *Math. Comput. Simul.* **55**, 271–280 (2001).

Acknowledgements

D.Z. and E.D.G. acknowledge the financial support from the European Research Council under the European Union's Horizon 2020 Research and Innovation Programme (agreement no. 682602, to E.D.G.). D.Z. also acknowledges support from the National Natural Science Foundation of China (grant no. 41988101). V.R.-G. acknowledges support from the European Research Council under agreement no. 771056.

Author contributions

D.Z. and E.D.G. conceived the study and model design. D.Z. built the model, performed the analyses and wrote the first draft. E.D.G. provided discussion and suggestions throughout the process. V.R.-G. and P.C. contributed to the interpretation of the results and writing of the manuscript.

Competing interests

The authors declare no competing interests.

Additional information

Supplementary information The online version contains supplementary material available at https://doi.org/10.1038/s41559-021-01548-3.

Correspondence and requests for materials should be addressed to Dan Zhu.

Peer review information *Nature Ecology & Evolution* thanks Trevor Fristoe and the other, anonymous, reviewer(s) for their contribution to the peer review of this work. Peer reviewer reports are available.

nature portfolio

Corresponding author(s): Dan Zhu

Last updated by author(s): Jul 17, 2021

Reporting Summary

Nature Portfolio wishes to improve the reproducibility of the work that we publish. This form provides structure for consistency and transparency in reporting. For further information on Nature Portfolio policies, see our Editorial Policies and the Editorial Policy Checklist.

Statistics

For all statistical analyses, confirm that the following items are present in the figure legend, table legend, main text, or Methods section.

n/a	Confirmed
☒	☐ The exact sample size (*n*) for each experimental group/condition, given as a discrete number and unit of measurement
☒	☐ A statement on whether measurements were taken from distinct samples or whether the same sample was measured repeatedly
☐	☒ The statistical test(s) used AND whether they are one- or two-sided *Only common tests should be described solely by name; describe more complex techniques in the Methods section.*
☐	☒ A description of all covariates tested
☐	☒ A description of any assumptions or corrections, such as tests of normality and adjustment for multiple comparisons
☐	☒ A full description of the statistical parameters including central tendency (e.g. means) or other basic estimates (e.g. regression coefficient) AND variation (e.g. standard deviation) or associated estimates of uncertainty (e.g. confidence intervals)
☒	☐ For null hypothesis testing, the test statistic (e.g. *F*, *t*, *r*) with confidence intervals, effect sizes, degrees of freedom and *P* value noted *Give P values as exact values whenever suitable.*
☒	☐ For Bayesian analysis, information on the choice of priors and Markov chain Monte Carlo settings
☒	☐ For hierarchical and complex designs, identification of the appropriate level for tests and full reporting of outcomes
☐	☒ Estimates of effect sizes (e.g. Cohen's *d*, Pearson's *r*), indicating how they were calculated

Our web collection on statistics for biologists contains articles on many of the points above.

Software and code

Policy information about availability of computer code

Data collection	no software was used in data collection.
Data analysis	Python was used to build the FORGE model, analyze the model outputs and plot the figures. R and SPSS were used to conduct the statistical analysis.

For manuscripts utilizing custom algorithms or software that are central to the research but not yet described in published literature, software must be made available to editors and reviewers. We strongly encourage code deposition in a community repository (e.g. GitHub). See the Nature Portfolio guidelines for submitting code & software for further information.

Data

Policy information about availability of data

All manuscripts must include a data availability statement. This statement should provide the following information, where applicable:

- Accession codes, unique identifiers, or web links for publicly available datasets
- A description of any restrictions on data availability
- For clinical datasets or third party data, please ensure that the statement adheres to our policy

The contemporary hunter-gatherer data and environmental variables used in the analysis are available in the supplementary materials.
Source code (in Python) of the FORGE model and its output files (in NetCDF format) for this study, including the three sets of global simulations (S0, S1, S2), are provided in a Supplementary zipped file. The corresponding input files for the FORGE model are deposited in the figshare repository: https://doi.org/10.6084/m9.figshare.14995320.v2

Field-specific reporting

Please select the one below that is the best fit for your research. If you are not sure, read the appropriate sections before making your selection.

☐ Life sciences ☐ Behavioural & social sciences ☒ Ecological, evolutionary & environmental sciences

For a reference copy of the document with all sections, see nature.com/documents/nr-reporting-summary-flat.pdf

Ecological, evolutionary & environmental sciences study design

All studies must disclose on these points even when the disclosure is negative.

Study description	We built a process-based hunter-gatherer dynamics model that is coupled to a pre-existing global terrestrial biosphere model, which simulates daily hunting and gathering activities of humans and the resultant carbon/energy flows among vegetation, herbivores and humans, and consequently the human population densities.
Research sample	The contemporary hunter-gatherer population densities and diet compositions were derived from existing datasets, as specified in Methods. The environmental variables at the location of the contemporary hunter-gatherer groups were extracted from the global gridded products, all specified in Methods.
Sampling strategy	All data points were included whenever available.
Data collection	The data were derived from published literature (sources specified in Methods) by the first author.
Timing and spatial scale	The original data were not collected by the authors.
Data exclusions	No data were excluded from the analyses.
Reproducibility	All the necessary data to reproduce this study are provided.
Randomization	Not relevant to this study since no experiments were carried out
Blinding	Not relevant to this study since no experiments were carried out

Did the study involve field work? ☐ Yes ☒ No

Reporting for specific materials, systems and methods

We require information from authors about some types of materials, experimental systems and methods used in many studies. Here, indicate whether each material, system or method listed is relevant to your study. If you are not sure if a list item applies to your research, read the appropriate section before selecting a response.

Materials & experimental systems

n/a	Involved in the study
☒	☐ Antibodies
☒	☐ Eukaryotic cell lines
☒	☐ Palaeontology and archaeology
☒	☐ Animals and other organisms
☒	☐ Human research participants
☒	☐ Clinical data
☒	☐ Dual use research of concern

Methods

n/a	Involved in the study
☒	☐ ChIP-seq
☒	☐ Flow cytometry
☒	☐ MRI-based neuroimaging